Simultaneous Noise Mitigation of Wavelength-multiplexed Signals by Self-tracking Passive Amplification

Benjamin Crockett[(1)*], Luis Romero Cortés[(1)], Reza Maram[(2)], José Azaña[(1)]
[(1)] *Institut National de la Recherche Scientifique (INRS) Montréal, Québec H5A 1K6, Canada,*
[(2)] *Fonex Data Systems Inc., Montréal, Québec H4S 1P6, Canada.*
**benjamin.crockett@inrs.ca*

Abstract: We demonstrate the self-tracking abilities of Talbot-based denoising by simultaneously processing 4 signals in a WDM scheme using a single device, without stabilization or alignment procedures, enabling significant BER and SNR improvements in all channels. 2022 The Author(s).

1. Introduction

A dedicated noise mitigation operation lies at the heart of nearly all telecommunication links [1]. Regardless of the specific characteristics of a given channel, the quality of the noise mitigation processes has a key role in the performance of a given fibre optics system. Ultimately, this is because the signal is gradually deteriorated through insertion loss, such that the signal under test (SUT) must undergo several amplification stages, most often using erbium-doped fibre amplifiers (EDFAs). This leads to the accumulation of important amounts of amplified spontaneous emission (ASE), which may even entirely drown the encoded information. Various noise mitigation schemes are thus employed to maintain the optical signal-to-noise ratio (OSNR) at acceptable levels [1].

By far the most common technique to denoise a noisy signal is the use of a bandpass filter (BPF). Even though optical BPF technologies have seen a tremendous improvement over the last few decades, they still possess significant drawbacks that renders them sub-optimal in many scenarios. For one, the design of optical BPFs with passbands below the GHz range remains a challenge [2], making them ill-suited for several important narrowband signal applications [3,4]. Most importantly, BPF approaches require that the frequency-domain specifications (e.g., central wavelength and bandwidth) of the SUT be known with high precision for optimal filtering. However, in practice the bandwidth of operation may change over time and the central wavelength may drift, such that the SUT's spectral properties may even need to be tracked in real time [5]. This is difficult in practice because BPF technologies often do not offer the needed reconfigurability. This is particularly important when the SUT is composed of multiple wavelength-multiplexed signals, such as in a Wavelength Division Multiplexing (WDM) system. In such scenarios, resonant structures are usually employed to filter the multiplexed signals, and it is generally difficult to design multiband filters with the needed customized features for optimal noise mitigation.

The issue with noise would be significantly alleviated if one could achieve truly noiseless amplification – or even better, denoising amplification. Phase sensitive parametric amplification has seen tremendous progress in recent years [6], with the potential for a 0 dB noise figure. However, they are difficult to implement in practice and it remains a major challenge to reliably fabricate fibre-optic parametric amplifiers with uniform transverse geometry over

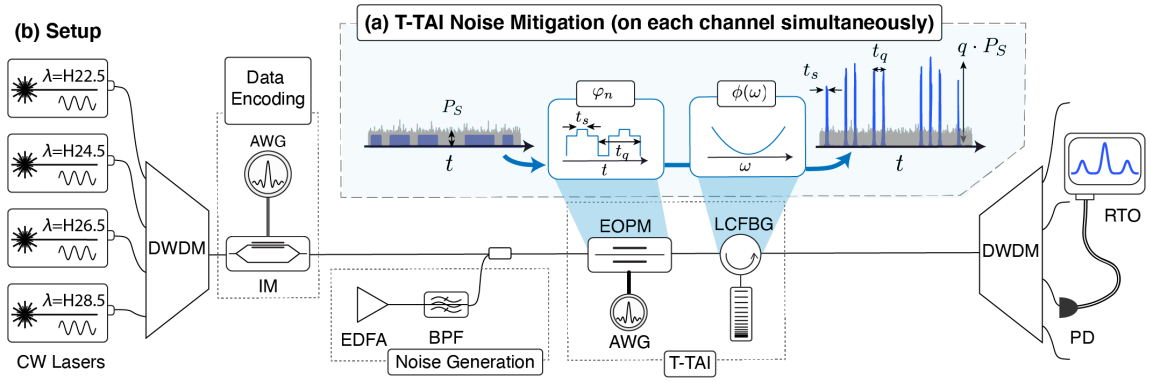

Fig. 1: (a) the T-TAI is composed of an electro-optic phase modulator (EOPM) driven by an electronic arbitrary waveform generator (AWG), followed by a linearly-chirped fibre Bragg grating (LCFBG) providing the needed second-order dispersive propagation. This redistributes the coherent part of a waveform (blue NRZ signal of power P_s buried under noise, grey, in the left temporal trace) into short pulses with an envelope corresponding to a copy of the input signal amplified by an integer factor q (blue peaks of width t_s in the right temporal trace, power $q \cdot P_s$). (b) Here we demonstrate the multi-wavelength capabilities of the T-TAI by processing 4 WDM signals at once. CW: Continuous wave, DWDM: Dense wavelength-division multiplexer/demultiplexer, IM: Intensity modulator, EDFA: Erbium-doped fibre amplifier, BPF: Bandpass filter, T-TAI: Temporal Talbot array illuminator, PD: Photodiode, RTO: Real-time oscilloscope.

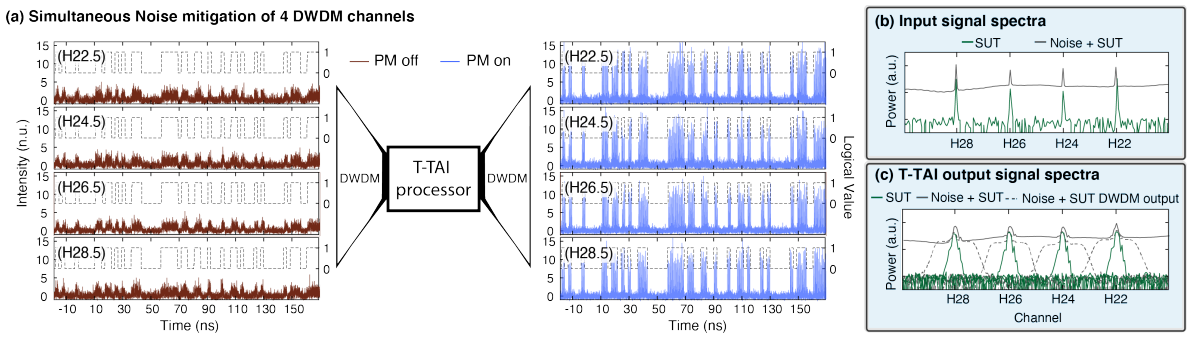

Fig. 2: (a) A single T-TAI mode allows to recover corrupted signals (PM off, red trace, left) by focusing the energy into short pulses outlining the input signal (PM on, blue trace, right). (b) the input signals (green trace) are degraded by injecting ASE noise (gray trace), effectively decreasing their OSNR. (c) All four channels are simultaneously processed, leading to the expected spectral broadening visible in the case without the injected noise (green trace). Part of the noise (gray trace) is inherently filtered out by the demultiplexing DWDM consisting of 100-GHz bandwidth pass-bands separated by 200 GHz (dashed gray trace).

hundreds of meters, leading to unpredictable dispersion fluctuations and efficiency variations [7]. Furthermore, any noise contained within the signal would also be amplified, such that dedicated noise mitigation stages may still be required. Recently, we have demonstrated passive amplification of optical waveforms based on the temporal Talbot array illuminator (T-TAI) concept [8,9], namely, the time-domain equivalent of the Talbot array illuminator [10]. This scheme relies on redistributing the coherent energy of a signal through a combination of temporal phase modulation and dispersive propagation, effectively causing the coherent SUT to be redistributed into a series of short pulses whose envelope follows an amplified copy of the input signal, see Fig. 1. In contrast, the incoherent noise contained along the input waveform is essentially unaffected by the phase manipulations, effectively decreasing the relative noise content of the waveform such that the signal can be recovered over the noisy background. We have demonstrated that this approach significantly outperforms an optical BPF [8]. A T-TAI performs the desired operation regardless of the SUT central wavelength; thus, as a key advantage, it has been anticipated that a T-TAI inherently tracks the signal's carrier frequency

In this communication, we provide an experimental demonstration of the self-tracking property of the T-TAI, and in particular, we show how this property can be exploited for processing multi-wavelength signals. Specifically, we propose and demonstrate that a single T-TAI module can perform the desired noise mitigation operation on multiple wavelength-multiplexed signals simultaneously, without any kind of spectral alignment or monitoring, offering a simple and straightforward technique for denoising WDM signals. This is demonstrated by simultaneously processing 4 multiplexed non-return-to-zero on-off keying (NRZ-OOK) pseudorandom binary sequences (PRBS). To show the versatility of the concept, we report successful significant noise mitigation of signals with varying OSNR and for two different data rates, namely 425 Mb/s and 1.7 Gb/s.

2. Principle of operation and experimental results

The basic implementation is shown in Fig. 1(a). In order to focus the waveform into peaks of width t_s, outlining a copy of the input waveform amplified by an integer factor q, the waveform first travels through an electro-optic modulator to imprint a specific temporal phase φ_n according to Talbot theory [11]. This phase is generated by an electronic AWG, and it is composed of discrete temporal levels of width t_s such that $\varphi_n = \text{-}\pi(q-1)n^2/q$, where n indexes the phase levels from 1 to q, leading to a periodic phase pattern repeating with a period $t_q = qt_s$ (q=4 depicted in Fig.1(a)). The modulated optical signal subsequently propagates through an amount of second order dispersion $|\ddot{\phi}|$ satisfying $2\pi|\ddot{\phi}| = qt_s^2$. The resulting output waveform can be interpreted as a copy of the input waveform amplified by a factor q that is sampled by short pulses of width t_s and with a period t_q.

In the reported experiments, the T-TAI was designed for $q = 12$ and $t_s = 48.9$ ps, yielding an output sampling rate of $1/t_q = 1.7$ GHz. As depicted in Fig. 1(a), this was implemented using a 40-GHz EOPM driven by a 24 GSa/s AWG, followed by a LCFBG with $|\ddot{\phi}| = 4{,}583$ ps^2. As shown in Fig. 1(b), the setup used for this experiment was composed of 4 CW signals centred at the DWDM ITU channels H22.5, H24.5, H26.5, and H28.5, corresponding to wavelengths of 1559.4, 1557.8, 1556.2, and 1554.5 nm, respectively. These signals were multiplexed using a DWDM module, and then an NRZ-OOK PRBS data signal with a bit length of 2^{10}-1 was encoded on all four carriers simultaneously using an electro-optic Mach-Zehnder intensity modulator. Note that a single modulator was employed simply for experimental convenience; in a real-world scenario, these signals would carry distinct data streams. Two

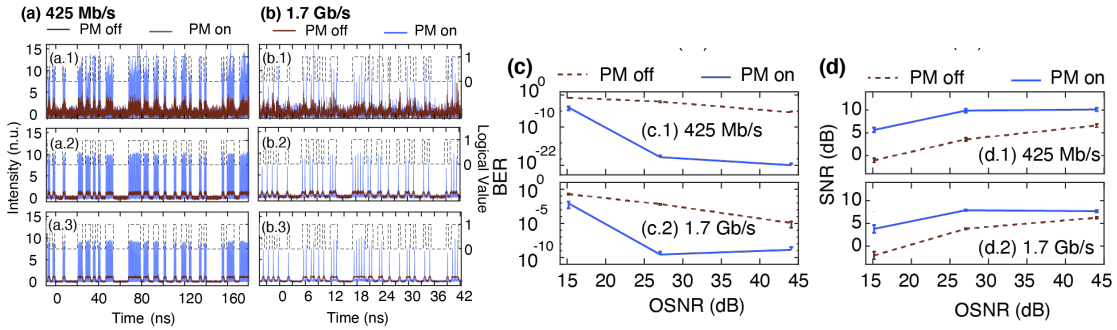

Fig. 3: The improvement in signal visibility is achieved for (a) the 425 Mb/s and (b) 1.7 Gb/s data signal, as the OSNR is varied from (1) 15.1 dB, (2) 27 dB to (3) 44 dB. (c) The BER and (d) SNR are found in each case, displaying a clear improvement in the SUT's noise characteristics.

signal bit rates were tested, namely 425 MB/s and 1.7 Gb/s, which result in 4 and 1 output TAI peaks per bit, respectively. These signals were then combined with ASE noise generated from a high-power EDFA, to test three levels of OSNR, namely 44.0, 27 and 15.1 dB, as measured by an OSA with a resolution of 0.01 nm. The corrupted signals were then simultaneously processed by the T-TAI module, without any need for spectral alignment or stabilization. Finally, the signals were demultiplexed using a second DWDM module, and each signal was measured individually using a 50-GHz PD connected to a 28-GHz RTO.

The multi-wavelength denoising effect of the T-TAI is illustrated in Fig. 2, for the case of the 425 Mb/s data signal with an OSNR of 15.1 dB. Upon a simple visual inspection of Fig. 2(a), it is clear that the denoising amplification effect of the T-TAI is achieved across all the tested wavelength channels. The improvement is quantitatively demonstrated below. Note that in order to accurately show the noise mitigation properties of the TAI (neglecting the inherent bandpass filtering occurring due to the DWDM modules), all waveforms were measured at the same location, namely after the second DWDM with the phase modulation (PM) on or off, Fig. 2(b-c). Fig. 3 summarizes the results of the TAI amplification for (a) the 425 Mb/s and (b) the 1.7 Gb/s data signal, in order of increasing OSNR. Here, only the waveforms centred at the channel H22 are shown for brevity. We document the quality of the signals by determining the Bit Error Rate (BER) and SNR. For each of the evaluated data rates and OSNR configurations, the mean value of the logical '1' μ_1 and '0' μ_0 values are found, as well as their corresponding standard deviations, σ_1 and σ_0. The BER is estimated from the well-known relation with the Q-factor, $BER = \mathrm{erfc}(Q/\sqrt{2})/2$, where $Q = (\mu_1 - \mu_0)/(\sigma_1 - \sigma_0)$ and erfc is the complementary error function [12]. The results are shown in Fig. 3(c) with the vertical axis in logarithmic scale. Here the advantage is most striking in the medium ONSR case (27 dB), giving an improvement in the BER by over 17 orders of magnitude for the case with the data rate of 425 Mb/s. We finish by finding the extracted SNR values, where $SNR = 10\log_{10}(Q)$, as commonly defined by eye diagram analysers [13], shown in Fig. 3(d). Once again, the T-TAI offers a significant improvement, which is most striking for the low OSNR waveform. For both the BER and the SNR, the error bars indicate the standard deviation across all 4 four channels, showing that the improvement is uniform across the channels.

4. Conclusion

We have shown that a single T-TAI module can be used to simultaneously mitigate the noise in multiple WDM signals, with quantitative significant BER and SNR improvements. We further note that the T-TAI can also be applied for complex modulation schemes such as QAM, and we predict that the T-TAI could be used in combination with envelop detection to conceive a practical detection stage offering an increased robustness against noise along a communication link.

5. References

[1] L.N. Binh, *Noises in Optical Communications and Photonic Systems*, Optics and Phototonics No. 14 (CRC Press, 2017).
[2] D.Marpaung, *et al.*, "Integrated microwave photonics," Nat. Phot. **13**, 80–90 (2019).
[3] C.V. Poulton, *et al.*, "Coherent solid-state LIDAR with silicon photonic optical phased arrays," Opt. Let. **42**, 4091–4094 (2017).
[4] J. Capmany, *et al.*, "Microwave photonic signal processing," JLT **31**, 571–586 (2013).
[5] J. Li, *et al.*, "Method for suppressing the frequency drift of integrated microwave photonic filters," Opt. Express **27**, 33575–33585 (2019).
[6] M.E. Marhic, *et al.*, "Fiber optical parametric amplifiers in optical communication systems: Fiber OPAs," Laser Photonics Rev. **9**, 50–74 (2015).
[7] L.K. Oxenløwe, *et al.* "Chapter 6 - Optical processing and manipulation of wavelength division multiplexed signals," in *Optical Fiber Telecommunications VII*, (Academic Press, 2020), pp. 233–299.
[8] B. Crockett, *et al.*, "Noise Mitigation of Narrowband Optical Signals Through Lossless Sampling," in *ECOC* 2019, Tu.2.C.4.
[9] B. Crockett, *et al.*, "Noise Mitigation of Random Data Signals Through Linear Temporal Sampling Based on the Talbot Effect," in *OFC 2019* M1B.2.
[10] A.W. Lohmann, "An array illuminator based on the Talbot-effect," Optik **79**, 41–45 (1988).
[11] C.R. Fernández-Pousa, "On the structure of quadratic Gauss sums in the Talbot effect," JOSA A **34**, 732–742 (2017).
[12] W. Freude, *et al.*, "Quality metrics for optical signals: Eye diagram, Q-factor, OSNR, EVM and BER," in *ICTON* 2012 pp. 1–4.
[13] Anritsu Corporation, "Understanding eye pattern measurements application note," (Application Note No. 11410-00533).